

## EVALUATION OF FRICTION STIR SPOT WELDED AL 5083 ALUMINIUM ALLOY AND C10100 COPPER DISSIMILAR JOINTS

S. Siddharth<sup>a\*</sup>, T. Senthilkumar<sup>a</sup>

<sup>a</sup>Department of Mechanical Engineering, University College Of Engineering, Bharathidasan Institute of Technology (BIT) Campus, Anna University, Tiruchirappalli - 620024, Tamil Nadu, India

\*Corresponding author, E-mail: sksmsiddharth1@yahoo.in, Phone. +91 0431 2511342, Cell. +91 7598651342.

Received: June 2016. Accepted: April 2017.

Published: December 2017.

### ABSTRACT

Friction stir spot welding (FSSW), a solid state joining process and a linear variant of Friction stir welding, has been used in industrial sectors for joining dissimilar materials like aluminium and copper alloys having different mechanical and metallurgical characteristics. In this paper, experimental evaluation of aluminium (Al) commercial alloy (Al 5083 – H111) and oxygen free copper (C10100) joints, using this technique, has been attempted, by varying the important process parameters such as tool rotational speed (RS) in rpm, plunging depth (PD) in mm and duration of dwell (DT) in seconds. Microstructural study using scanning electron microscopy was conducted to evaluate the mixing of the base materials in the weld interface. The grain structure and morphological changes were studied to predict the effect of stir. The effect of process parameters on the tensile shear failure load of joints were observed. Energy-dispersive X-ray spectroscopy was used for evaluating intermetallic compounds at joint interface. The presence of intermetallic compound AlCu was detected at the joint interface, formed during FSSW process at parameters RS-1250 rpm, DT-12 sec, PD-2.1 mm. The interface regions were found to be a finely fused combination of aluminium and copper in most of the regions and chaotic in certain places.

**Keywords:** Friction stir spot welding; aluminium; copper; dissimilar materials; microstructure.

### EVALUACIÓN DE UNIONES DISIMILARES DE ALUMINIO (AL5083) Y COBRE (C10100) MEDIANTE SOLDADURA POR FRICCIÓN

#### RESUMEN

Soldadura fricción revuelo (FSSW) se une a los materiales sin la fusión. Puede ser utilizado para unir diferentes materiales con diferentes propiedades mecánicas y metalúrgicas. Se utiliza para unir materiales como aluminio y cobre. En esta investigación, el aluminio (AL5083) y el cobre (C10100) se unieron utilizando este método. Se cambió la velocidad de rotación de la herramienta (RS), profundidad de inmersión (PD) y tiempo de permanencia (DT). Se realizó un estudio microestructural utilizando microscopía electrónica de barrido para evaluar la mezcla de los materiales base en la interfase de soldadura. La estructura del grano y los cambios morfológicos fueron estudiados para predecir el efecto de agitación. El efecto de los cambios en los parámetros FSSW se estudiaron. Se usó espectroscopia de rayos X de dispersión de energía para encontrar los compuestos intermetálicos. La presencia del compuesto intermetálico AlCu se detectó en la interfase de unión, formada durante el proceso FSSW a los parámetros RS-1250 rpm, DT-12 seg, PD-2,1 mm. Se encontró que las regiones de interfaz eran una combinación finamente fundida de aluminio y cobre en la mayoría de las regiones y caótica en ciertos lugares.

**Palabras claves:** Fricción revuelo soldadura por puntos; aluminio; cobre; materiales diferentes; microestructura.

#### INTRODUCTION

Friction Stir Welding (FSW) is a solid-state material joining technique developed and patented in 1991 by The Welding Institute, Cambridge, England [1]. Friction Stir Spot Welding (FSSW) is its linear variant used to join

different materials for industrial applications. Frictional heat is introduced by plunging a non-consumable rotating tool into the weld spot. For a certain period of dwell time it is held at that position and then the tool is retracted,

allowing the softened region to cool and form a friction stir spot weld [2]. It is a three-step process involving (a): Plunging: Plunging of the non-consumable rotating tool, (b): Stirring: The tool is allowed to stir the weld zone for a specific duration and (c): Drawing out: Tool is removed from the weld zone to allow the joints to cool [3]. The schematic representation of the FSSW process is shown in Fig. 1.

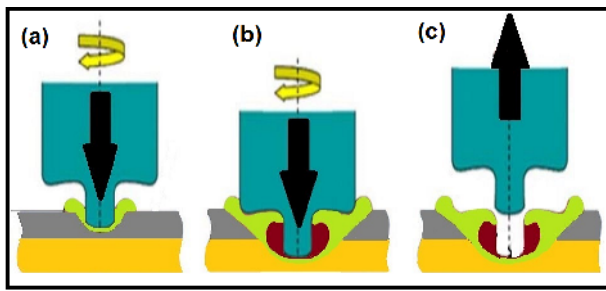


**Fig 1.** Schematic representation of the three phases of FSSW process: (a) plunging, (b) stirring and (c) retracting

The cross section of a typical FSSW joint shown in Fig. 2 indicates five characteristic features that include (i) Parent Material (PM): Unaffected nor deformed base material, (ii) Heat Affected Zone (HAZ): Region closer to weld area with modified microstructure but no plastic deformation, Thermo-mechanically Affected Zone (TMAZ): Region where plastic deformation has occurred due to frictional heat and stir induced by tool, Stir Zone (SZ): Completely recrystallized region surrounding the tool pin, Hook: A distinct FSSW feature at the joint interface for origination of geometrical defects [4].

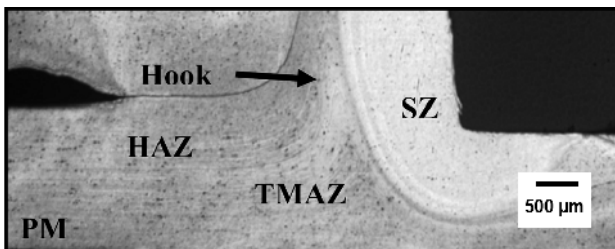


**Fig. 2.** Cross section of typical FSSW joint

Many research investigations had been conducted in joining similar and dissimilar materials using FSSW

techniques. Tozaki *et al.*, investigated the FSSW process parameters of aluminium alloy 6061-T4 sheets with probe-less tool and observed that when stir zone is small, shear fracture of the nugget takes place leading to lower tensile shear failure load [5]. Hong *et al.*, joined dual phase steel (DP780GA) and hot stamped boron steel (HSBS) sheet using FSSW technique and observed that increase in rotational speed led to a) increase in breaking load value, b) more heat generation and c) increase in the size of the stir zone and the bonded area [6]. Akinlabi *et al.*, friction stir welded 5754 aluminium alloy and C11000 copper and characterized the fracture surfaces and found the presence of intermetallic compounds which affected the weld quality [7]. Rostamiyan *et al.*, joined AA6061 using FSSW and analyzed its weld quality using scanning electron microscopy (SEM). It was observed that introduction of ultrasonic vibrations during the FSSW process resulted in a uniformly distributed and a finer grain structure [8]. Mukuna *et al.*, joined AA1060 and C11000 using FSSW process and found distinct copper rings formation in the aluminium matrix with good material mixing during microstructural evaluation [9]. Ugur *et al.*, joined aluminum alloy 1050 and pure copper using FSSW technique and found the influence of intermetallic phases on tensile properties and hardness [10]. Heiderman *et al.*, successfully produced FSSW joints with 6061 Al-T6 aluminium and a 1.5 mm copper without intermetallic compounds [11]. In this study, the mechanical and metallurgical characteristics of FSSW joints of Al 5083 aluminium and C 10100 copper alloy have been investigated.

## MATERIALS AND METHODS

In this study, (as per ASM standards) Al 5083 – H111 aluminium (Al) commercial alloy sheet of 1.5 mm thickness and (as per JIS standards) C10100 oxygen free copper of 1.5 mm thickness were used. The chemical composition of the base materials is given in Table 1 and its important mechanical properties are shown in Table 2.

**Table 1.** Nominal chemical composition of the base materials (wt. %)

AL 5083 = Si-0.4, Mg-4.0, Mn-0.4, Fe-0.4, Cr-0.25, Cu-0.1, Zn-0.25, Ti-0.15, Al-Balance
C10100 = Pb-0.003, Sn-0.002, S-0.004, Fe-0.004, Zn-0.003, O-0.002, P-0.002, As-0.002, Cu-Balance

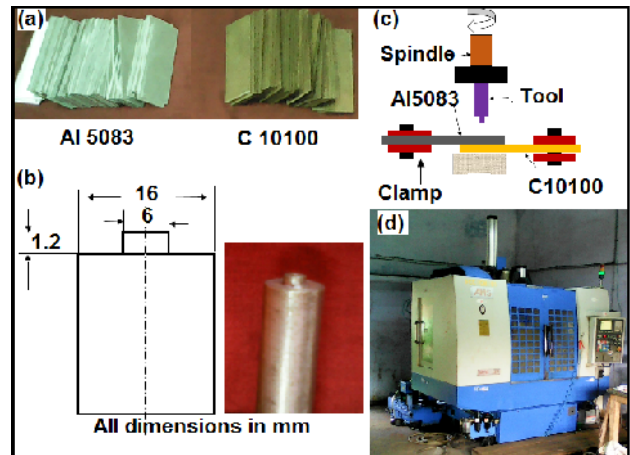
**Table 2.** Important mechanical properties of the base materials.

Yield Str. - Tensile Str. - Elongation - Hardness
Al5083 - 145 MPa - 290MPa - 22% - 87 HV
C10100- 275 MPa -310 MPa - 20% - 75 HV

The base materials are shown in Fig 3(a). The work pieces were machined to dimensions of 30 mm breadth and 100 mm length. 30 mm overlap was given for the joints, placing aluminium alloy on top and copper on the bottom. When thin sheets are joined by FSSW, most of the frictional and deforming heat arise from tool shoulder for both surface and subsurface [12]. Cylindrical, straight tool for FSSW welds were made with H13 tool steel, with shoulder diameter 16 mm, pin diameter 6 mm with pin length 1.2 mm (Fig. 3. (b)). The configuration of FSSW setup is shown in Fig. 3. (c), and the equipment (Ace Micromatic AMS MCV – 450) used for welding the joints is shown in Fig. 3. (d). The microstructures were examined by scanning electron microscopy (SEM) (Make - Penta FET precision with OXFORD 10mm<sup>2</sup> SDD Detector - x-act). TESCAN instrument with Vega TC software was used for SEM analysis. Standard specimen preparation methods were used [13].

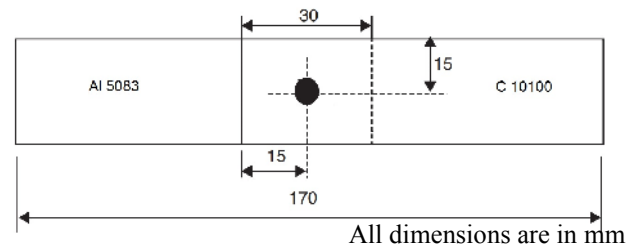
The important process parameters influencing the overall strength and quality of joints are tool rotation speed (RS) in rpm, plunge depth (PD) in mm and dwell time (DT) in sec [14]. Within feasible limits of the process parameters found by trial experiments, the joints were made. The samples were surface cleaned to remove dirt and wiped

with acetone before clamping for weld. In Table 3, the surface macrographs of a few welded samples are shown.

**Fig. 3.** (a) Sized base materials Al 5083 and C10100, (b) Tool nomenclature, (c) Configuration of FSSW setup, (d) FSSW machine.

## RESULTS AND DISCUSSION

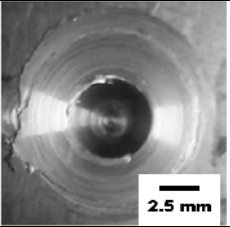
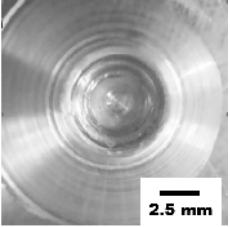
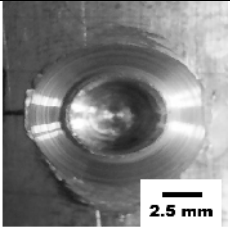
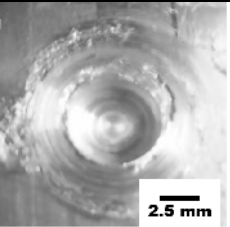
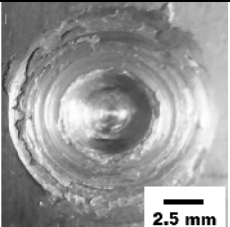
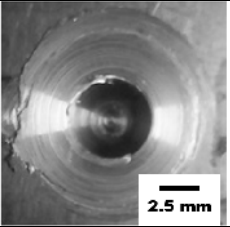
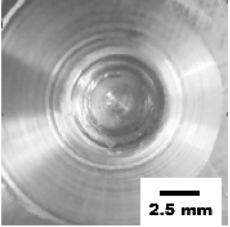
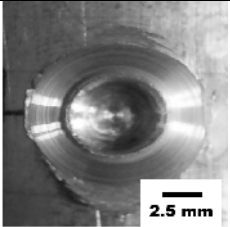
Tensile fracture specimens were prepared as shown in Fig. 4.

**Fig. 4.** Specimen nomenclature for fracture tests.

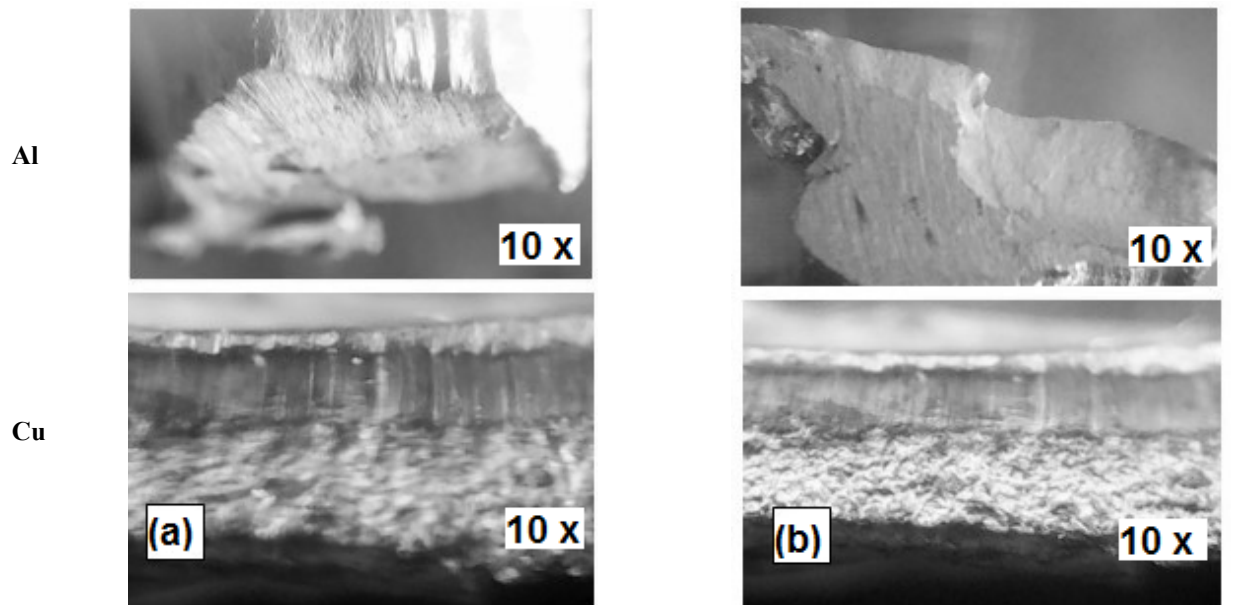
Electromechanically controlled Universal Testing Machine (FIE-Bluestar, India; model UNITEK-94100), of 100-kN capacity was used for finding the tensile shear failure loads (TSFL). As per ASTM specifications the specimens were loaded at the rate of 1.5 kN/min till failure of the joints. The properties of FSSW joints depends upon the annular bond area and metallurgical bond at the joint interface region. The fracture regions of certain FSSW joints with 10 x magnification were examined (Fig. 5).

Fig 5 (a) indicates the fractured cross sectional view of the joint (RS - 1500 rpm, DT - 7 sec, PD - 1.4 mm) in which Al is found to have a finer grained region. The deformation of the top plate is effected by the vertical and horizontal push of the softened materials. This causes pile up of the Al material which is observed on the top right corner. The effect of the stir on the bottom Cu plate is observed. A finer grain pattern is observed on the top side of the bottom Cu plate which had undergone high thermal cycles and the bottom side of Cu plate is coarser. Fig 5 (b) indicates the cross-sectional view of the fractured region at S - 1250 rpm, DT - 12 sec, PD - 2.1 mm. In the top Al plate on the left side, the accumulation of the softened material is observed. The overall region is fine owing to the softening which it has experienced due to the interaction with the tool. The bottom Cu plate is found to have a boundary above which the grains are fine owing to the annealing effect caused by the frictional effect of the tool and the region below the boundary is coarse grained. Fig 5 (c) indicates the sectional view of the fractured region at RS - 1000 rpm, DT - 15 sec, PD - 2.4 mm. In the top Al side, the alignment of the softened materials along the tool rotational direction is observed.

**Table 3.** Surface morphologies of Al/Cu FSSW at different welding parameters

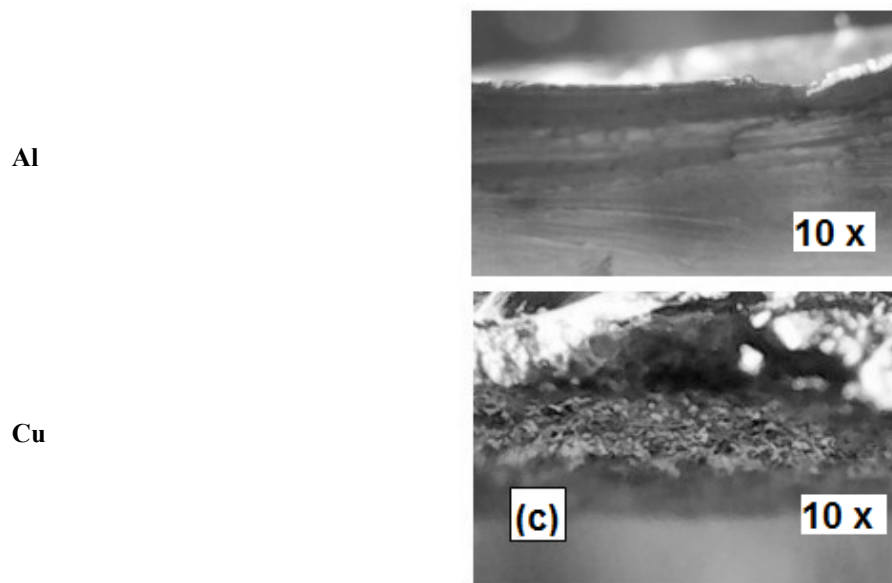
Specimen 1			
RS - 1000			
DT - 15			
PD - 2.4			
Keyhole			
Width	Height		
5.6	2.3		
Flash - 0.1			
Specimen 2			
RS - 1150			
DT - 14			
PD - 2.2			
Keyhole			
Width	Height		
5.6	2.2		
Flash - 0.2			
Specimen 3			
RS - 1250			
DT - 12			
PD - 2.1			
Keyhole			
Width	Height		
5.2	1.8		
Flash - 0.6			
Specimen 4			
RS - 1300			
DT - 9			
PD - 1.8			
Keyhole			
Width	Height		
5.1	1.6		
Flash - 0.8			
Specimen 5			
RS - 1500			
DT - 7			
PD - 1.4			
Keyhole			
Width	Height		
4.8	1.2		
Flash - 1.1			

RS in rpm, DT in seconds, PD in mm, Keyhole width, Keyhole diameter and Flash rise in mm



(a) At RS - 1500 rpm, DT - 7 sec, PD - 1.4 mm

(b) At RS - 1250 rpm, DT - 12 sec, PD - 2.1 mm



(c) At RS - 1000 rpm, DT - 15 sec, PD - 2.4 mm

**Fig. 5.** Fracture zones of top Al and bottom Cu plates made with pinned tool.

In the bottom, Cu region, excessive tear and rupture were observed. The action was found to be more of mechanical shear and deformation due to higher plunge depth of the tool and lower tool speed. Heideman *et al.*, observed certain similar changes in the grain pattern of Al and Cu at the weld zones of FSSW joints [11]. Location of fracture was between stir zone (SZ) and thermo-mechanically affected zone (TMAZ). Irregular uneven surface was observed with coarse granular surfaces. Al 5083 side was fine grained than bottom copper plate. Thin layer of fine granular structure was found at top portion of C10100 which comes in direct contact with FSSW tool and coarse granular structure was found in the remaining portion (Fig. 5). Size of the stir zone increases with increase in rotational speed due to increased stir. The failure modes observed were *interfacial* (fracture at joints) and *nugget pullout* (sheet tear off) due to the effect of changes in the process parameters. Similar fractures were observed by Lakshminarayanan *et al.*, [15]. The tensile shear failure loads of the specimens with type of fracture under various process parameters are presented in Table 4.

**Table 4.** Tensile data

Specimen	Parameters			TSFL (kN)	Fracture type
	RS	DT	PD		
1	1000	15	2.4	0.89	Interfacial
2	1150	14	2.2	0.92	Interfacial
3	1250	12	2.1	1.12	Nugget pullout
4	1300	9	1.8	1.04	Nugget pull out
5	1500	7	1.4	0.96	Interfacial

The microstructures were examined by scanning electron microscopy (SEM). The microstructure of specimen 3 of Table 4 was analyzed. The unaffected parent material (PM) (more than 18 mm away from the weld center) microstructure of Al – 5083 – H111 (Fig. 6 (a)) consisted of coarse second-phase particles and fine grain boundary

precipitates which were equiaxed. It could be attributed to rolling of plates for elongation of grains. The parent base material (PM) of C 10100 (Fig 6 (b)) consisted of a small tree like sparsely reduced dendrites which were nearly eliminated due to rolling.

In the heat affected zone (10 mm away from weld center) (HAZ) of Al 5083 (Fig 6 (c)), the precipitate concentration in grain boundaries defined the grains. Inter-granular with trans-granular precipitates were observed. Owing to the heat from the frictional stir, due to dislocation polygonization, partial sub-grains formation was observed. Certain recovery characteristic involving rearrangement of dislocations and nearly equiaxed fresh fine grains could also be observed.

In the heat affected zone of C 10100 (Fig 6 (d)), more parallel straight lines extending across many of the grains could be seen that presented with small dimples distributed owing to the frictional heating.

The thermos-mechanically affected zone (TMAZ) (region adjacent to stir zone) of Al 5083 shown in Fig. 6 (e) had undergone distinct changes in grain structure due to excessive heat flow. Deformed pancake grains witnessed elongation and rotation due to the high strain they were subjected to. The thermos-mechanically affected zone (TMAZ) of C 10100 is given in Fig. 6 (f). The material flow was determined by the plunge and rotation of the tool.

The high temperature reached in the zone influenced the grain structure. The material was likely to undergo complete recrystallization close to the nugget zone. The deformation increases with proximity towards nugget interface.

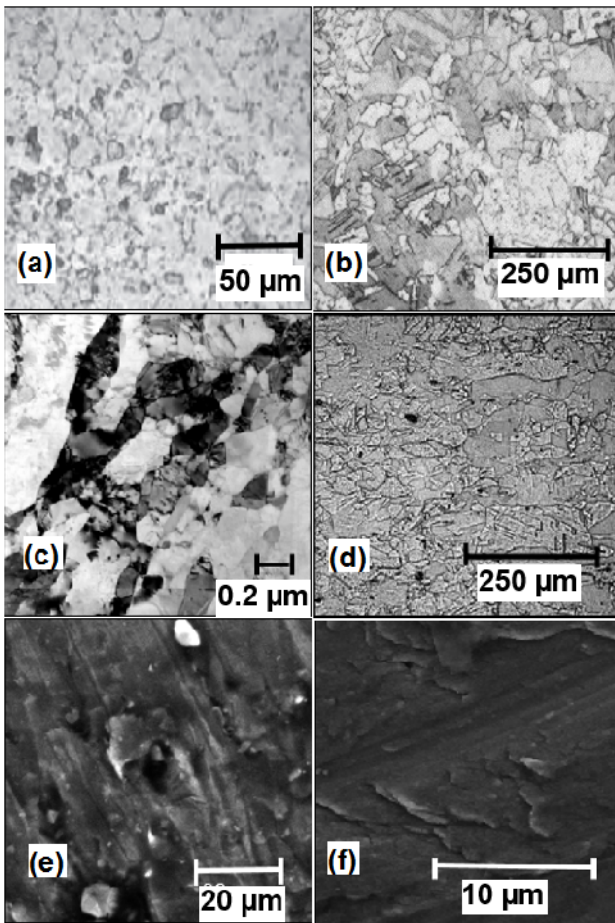


**Fig. 6.** FSSW joints at RS-1250 rpm, DT-12 sec, PD-2.1 mm, Microstructures of - Parent material (a) Al 5083, (b) C10100, Heat Affected Zone - (c) Al 5083, (d) C10100, TMAZ – (e) Al 5083 & (f) C10100.

There is an evident boundary between Al 5083 and Cu 10100, observed at the stir zone below the shoulder (Fig 7 (a)), at 973 x magnification for Specimen 3. The grain structure of copper alloy was found to be more equiaxed and fine grained than that of aluminum. At 2.4 kx magnification (Fig. 7 (b)), deformed flakes in the copper region around size of 5 to 7  $\mu\text{m}$  were observed in Specimen 5, which could act as crack initiation regions, responsible for decrease in weld strength. The porosity in aluminium zone is more pronounced.

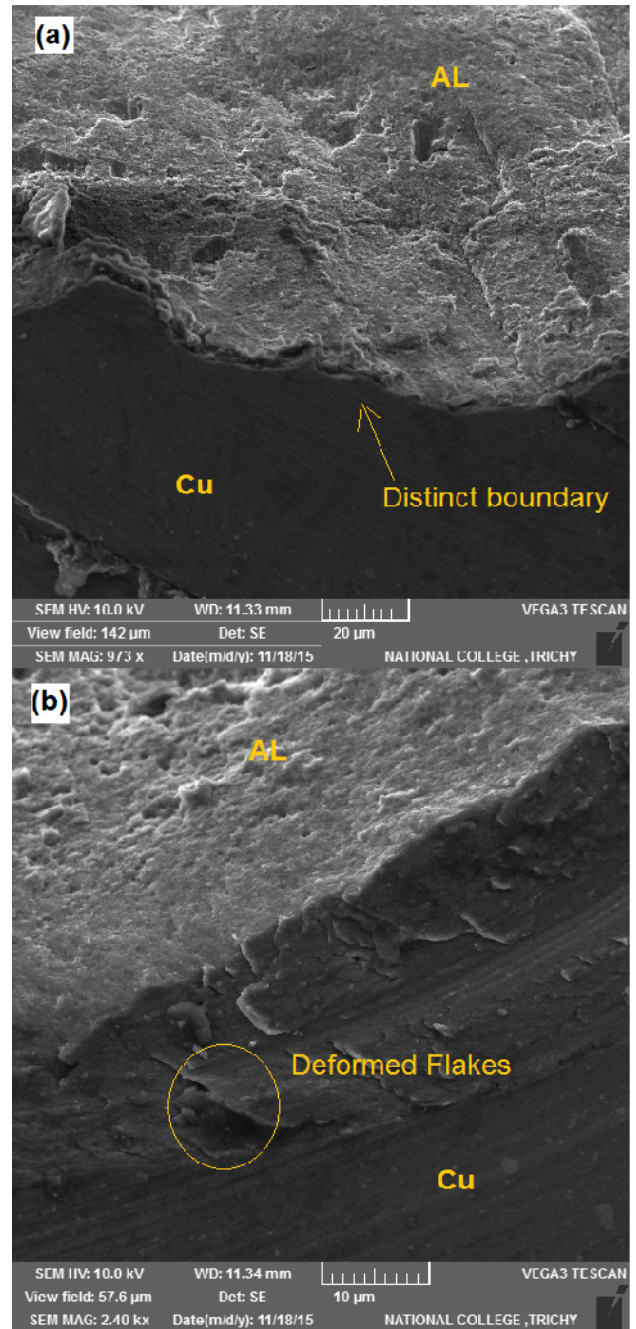


**Fig. 7.** Microstructure of the Stir Zone (SZ) directly under tool shoulder (a) Specimen 3 at RS-1250 rpm, DT-12 sec, PD-2.1 mm, and (b) Specimen 5 at RS-1500 rpm, DT-7 sec, PD-1.4 mm.

SEM image of 3<sup>rd</sup> specimen, at 6.41 kx magnification of SZ under tool pin, (Fig 8 (a)), indicates that aluminum and copper were sufficiently mixed due to the stirring process. Improper chaotic structures that are mixed, repel the bonding contribution of mechanical interlocking effect. At 4.5 kx magnification, (Fig 8 (b)), distribution

of fine aluminium grains over the copper region were observed at stir zone under tool pin for specimen 5.

Distribution of sufficiently intermixed aluminium and copper was observed along the tool rotation direction, irrespective of the parent rolling direction of the base materials. In Fig. 9. (a) SEM image for spectrum analysis for finding the interface components (Specimen 3) is shown. The presence of intermetallic compounds accounts for brittleness of the joints thereby reducing the overall strength of the joints.

The peaks of the spectrum analysis of the interface region (energy dispersive X-ray spectroscopy analysis of specimen 3) is given in Fig 9 (b). The predominant components observed were aluminium and copper. The actual weight and atomic percentage resulted from spectrum processing are given as follows

Element	Weight %	Atomic %
C K	5.32	12.71
O K	1.26	2.25
Al K	69.62	74.03
Si K	0.36	0.37
Mn K	0.25	0.13
Fe K	0.88	0.45
Cu K	20.70	9.35
Zn K	1.62	0.71
Total	100.00	

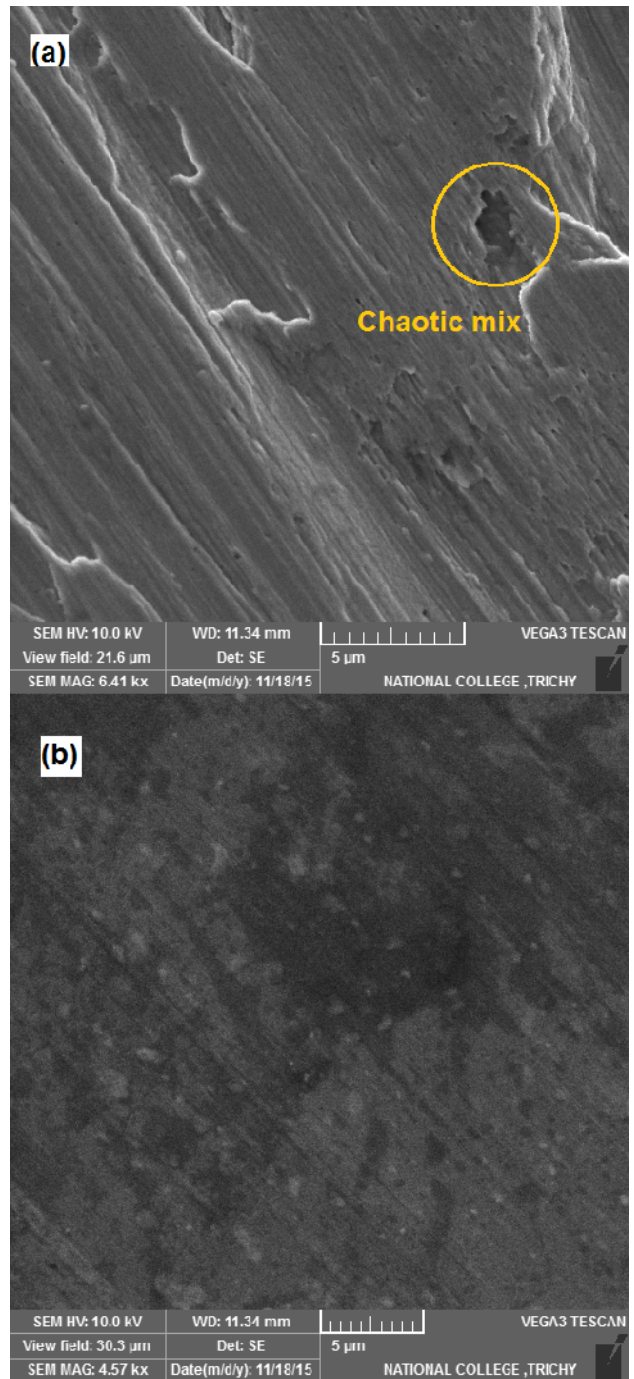


**Fig. 8.** Microstructure of the Stir Zone (SZ) directly under pin **(a)** Specimen 3 at RS-1250 rpm, DT-12 sec, PD-2.1 mm, and **(b)** Specimen 5 at RS-1500 rpm, DT-7 sec, PD-1.4 mm

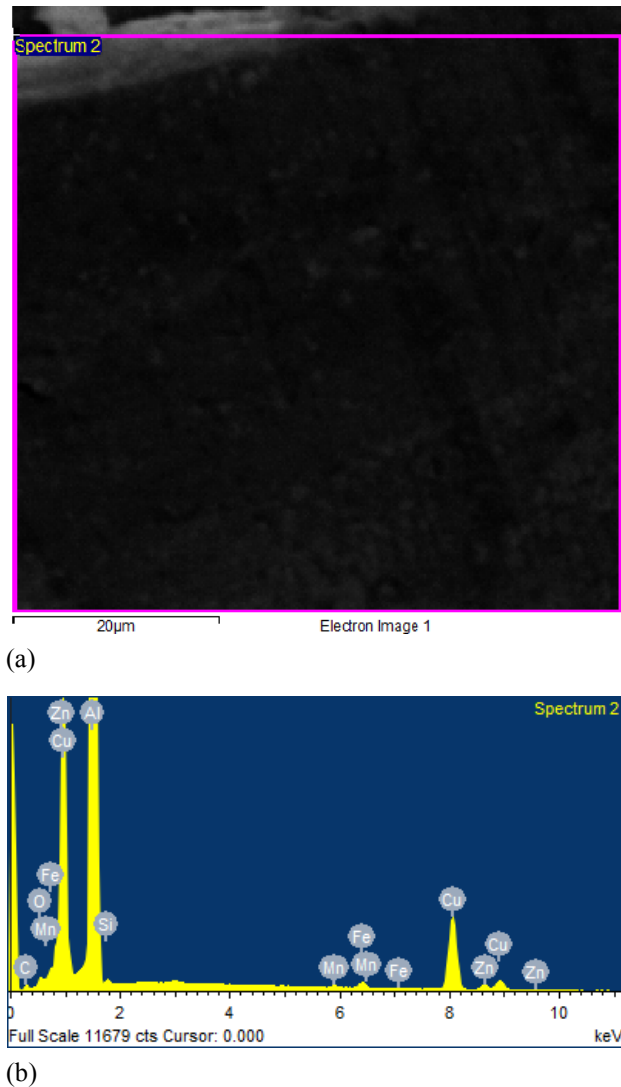


**Fig. 9. (a)** SEM Image of Specimen 3 at stir zone for spectrum analysis, **(b)** Analysis of spectrum 2 of SEM image of specimen 3.

Owing to the differences in coefficient of thermal expansion formation of solid solutions at the weld interface of dissimilar materials can be attributed to the formation of intermetallic compounds [16].

The percentage of the components were correlated with Aluminium-Copper (Al-Cu) Binary phase diagram [17] and the interface region were found to be composed of AlCu at 595°C.

## CONCLUSIONS

Thus, friction stir spot welding (FSSW) of dissimilar aluminium alloy Al 5083 and copper C10100 were conducted and effect of the important process parameters such as tool rotational speed (RS), dwell time (DT) and plunge depth (PD) on mechanical and microstructural variations were observed.

i) At higher tool speed (RS) of, RS - 1500 rpm, DT - 7 sec, PD - 1.4 mm a thin layer of fine grains close to Al/Cu interface and remaining coarsely grained region were observed at fractured C10100 region due to annealing effect of the tool, whereas at lower tool speed of 1000 rpm, DT - 15 sec, PD - 2.4 mm excessive tear and rupture were observed due to shear deformation

ii) At RS-1250 rpm, DT-12 sec, PD-2.1 mm, a distinct boundary was observed at the interface of the weld region separating aluminium and copper.

iii) Grains closer to weld zone were more thermally affected owing to partial sub-grains formation. At the thermo-mechanically affected (TMAZ) zones for joints made at RS-1500rpm, DT-7sec, PD-1.4mm, grains were pancake shaped in Al side and copper granules were deformed to form flakes around 5-7 µm in length. These flakes could act as a source for crack initiation.

iv) At stir zone of joints made at RS-1250 rpm, DT-12 sec, PD-2.1mm, finely fused distribution of copper and aluminium was observed at the interface. Chaotic mix at certain regions was also found.

v) At interface of joint made at RS-1250 rpm, DT-12 sec, PD-2.1 mm, Energy dispersive X-ray spectroscopy indicated the presence of intermetallic compound AlCu due to solid solution formation at bottom region of top Al5083 and top region of bottom C10100.

## REFERENCES

- [1] Thomas W. M., Nicholas E. D., Needham J. C., Murch M. G., Templesmith P., C. J. Dawes C. J.

- (1991) "Improvements relating to Friction Welding" Patent N. PCT/GB92/02203
- [2] Harsha Badarinarayan (2009) "Fundamentals of friction stir spot welding" PhD thesis, *Missouri University of Science and Technology, United States.*
- [3] Hovanski Y., Santella M. L., Grant G.J. (2007) "Friction stir spot welding of hot-stamped boron steel" *Scripta Materialia* 57: 873–876.
- [4] Badarinarayan H., Yang Q., Zhu S. (2009) "Effect of tool geometry on static strength of friction stir spot-welded aluminum alloy" *International Journal of Machine Tools and Manufacture* 49(2): 142-148.
- [5] Tozaki Y., Uematsu Y., Tokaji, K. (2010) "A newly developed tool without probe for friction stir spot welding and its performance" *J. Mater. Process. Technol.* 210: 844 – 851.
- [6] Hong, Sripichai S., H., Yu K., Avery C., S., Pan K., Pan T. (2012) "Failure modes of friction stir spot welds in lap-shear specimens of dissimilar advanced high strength steels under quasi-static and cyclic loading conditions" *SAE International Journal of Materials and Manufacturing* 5: 375–381
- [7] Akinlabi, Esther T., Stephen A. (2014) "Friction stir welding of aluminium and copper: Fracture surface characterizations" *World Congress on Engineering, London, U.K. (II)*: 1525- 1528.
- [8] Rostamiyan Y., Seidanloo A., Sohrabpoor H., Teimouri R. (2015) "Experimental studies on ultrasonically assisted friction stir spot welding of AA6061" *Archives of Civil and Mechanical Engineering* 15: 335 – 346
- [9] Mukuna P. Mubiayi, Esther T. Akinlabi (2015) "Friction Stir Spot Welding between Copper and Aluminium: Microstructural Evolution", *Proceedings of the International Multi-Conference of Engineers and Computer Scientists IMECS 2015, Hong Kong (II)*: 819-823.
- [10] Ugur Ozdemir, Sami Sayer, Çinar Yeni, Bornova Izmir (2012) "Effect of Pin Penetration Depth on the Mechanical Properties of Friction Stir Spot Welded Aluminum and Copper" *Materials Testing in Joining Technology* 54: 233-239.
- [11] Heideman R., Johnson C., Kou S. (2010) "Metallurgical analysis of Al/Cu friction stir spot welding" *Science and Technology of Welding and Joining* 15(7): 597-604
- [12] Byung Wook A., Chang Yong L., Don Hyun C. (2010) "Effect of Pin Shapes on Joint Characteristics of Friction Stir Spot Welded AA5J32 Sheet" *Materials transaction* 51(5): 1028- 1032.
- [13] E3-11 Standard Guide for Preparation of Metallographic Specimens (2011), *Annual book of ASTM Standards volume International.*
- [14] Tozaki Y., Uematsu Y., Tokaji, K. (2010) "A newly developed tool without probe for friction stir spot welding and its performance" *J. Mater. Process. Technol.* 210: 844 – 851.
- [15] Lakshminarayanan A.K, Annamalai V.E., Elangovan K (2015) "Identification of optimum friction stir spot welding process parameters controlling the properties of low carbon automotive steel joints", *Journal of Materials Research and Technology*, Vol. 4, no. 3, pp. 262-272.
- [16] Jian Zhang, Qiang Shen, Guoqiang Luo, Meijuan Li and Lianmeng Zhang (2012) "Microstructure and bonding strength of diffusion welding of Mo/Cu joints with Ni interlayer" *Materials Design* 39: 81-86.
- [17] Nbnbn Massalski T., B., Okamoto H., Subramanian P. R., Kacprzak L. (1990) "Binary alloy phase diagrams" *ASM International, Ohio, USA* :141-143.